Optimal Sizing of Onboard Hybrid Energy Storage Devices Considering the Long-Term Train Operation

BOLUN ZHANG [1], **CHAOXIAN WU**[2], **GUANGZHAO MENG**[1], **FEI XUE** [3], **AND SHAOFENG LU** [1]

[1]Shien-Ming Wu School of Intelligent Engineering, South China University of Technology, Guangzhou 510000, China
[2]School of Systems Science and Engineering, Sun Yat-sen University, Guangzhou 510000, China
[3]School of Advanced Technology, Xi'an Jiaotong-Liverpool University, Suzhou 215000, China

Corresponding author: Shaofeng Lu (lushaofeng@scut.edu.cn)

ABSTRACT With the fast development of energy storage technology, more applications of Energy Storage Devices (ESDs) have been found in rail transportation in recent years. This paper aims to address the optimal sizing problem of on-board Hybrid Energy Storage Devices (HESDs) which are installed to assist train traction and recover the regenerative braking energy. On-board HESDs combining Li-ion battery and supercapacitor can further enhance the capacity and instant power rating. In this paper, a mixed integer linear programming (MILP) model is proposed to minimize the economic cost in terms of energy consumption and installation, and the degradation cost of on-board HESDs considering the long-term train operation constrained by the initial investment of on-board HESDs. Train operation is found to be highly related to characteristics of on-board HESDs including the maximum power, capacity, and state of health (SOH). By changing the investment ratio between Li-ion battery and supercapacitor, the energy-saving rate and economic cost for various investment ratios have been obtained. Compared with the results of train optimal control with Li-ion battery only, supercapacitor only and no on-board HESDs, the results indicate an energy-saving rate up to 25.59%, from the perspective of the long-term train operation. When the allowable capital cost is relaxed from 20 k\$ to 60 k\$, the cost per kilometer is reduced from 0.55 USD/km to 0.53 USD/km, showing higher capital cost is closely linked to higher cost reduction in the long-term train operation.

INDEX TERMS Optimal sizing, mixed integer linear programming (MILP), on-board hybrid energy storage device (HESD), the long-term train operation.

I. INTRODUCTION

Compared with other modes of transportation, electrified rail transportation has advantages of large capacity, punctuality, and environmental friendliness. The recent increase in worldwide interest in improving the energy efficiency of railway systems has led to an increase in associated planning, investment, and construction costs. Nowadays the optimal use of energy storage devices (ESDs) to recover more regenerative energy and improve traction efficiency has attracted growing attention [1].

The associate editor coordinating the review of this manuscript and approving it for publication was Kuo-Ching Ying [iD].

Differernt types of ESDs are commonly utilized in electrified railway systems, namely batteries (BATs), flywheels and supercapacitors (SCs). BATs are well known for their high-energy density and large energy-storage capability. Due to this characteristic, although BATs remain the popular choice to absorb the regenerative energy in some electrified sections, they pose important constraints such as energy efficiency and the limited number of cycles [2], [3]. Concerning SCs, they can achieve higher power density, much larger number of cycle lifetime, and cycling efficiency. However, taking into account the state of technology, the high price and low energy density hamper their cause [4]. With regard to flywheels, the main disadvantages include maintenance costs, extra weight and cost for high-speed types [5]. Fuel

cells (FCs) are other attractive energy sources. Although the FCs technology is very promising, it still faces many challenges associated with hydrogen storage and refueling [6]. Given the current situation of ESDs, a single class of them is difficult to offer features in modern electrified railway systems, such as long cycle lifetime, reasonable cost, and appropriate power and energy densities [7]. Consequently, the hybrid energy storage devices (HESDs), combining both SCs and BATs, have an enhanced ability in capturing the high-power regenerative braking energy using SCs and an extended lifetime of BATs [8], [9].

Many existing papers have reported the use of ESDs to recover and reuse energy during regenerative braking, and the application of ESDs is being widely studied. Once the driving strategies are found, it can be proved that the energy consumption in the urban rail systems through installing ESDs could be reduced by approximately 25-35% [10]. In [11], the design of a novel optimization method based on genetic algorithm and a simulation platform has been proposed, which aims to use SCs to recovery regenerative braking energy and improve the pantograph voltage profile. The proposed method was implemented by controlling the voltage or state-of-charge of ESDs for recycling the regenerative braking energy, which were verified by experimental tests and the simulations [12]. In [13], the authors presented that the total energy consumption of the train can be reduced by optimizing the train speed profiles and the charging and discharging control signal of the ESDs when the train was braking or accelerating. Wu *et al.* [14] and Wu *et al.* [15] investigated a novel integrated MILP model to co-optimize train speed profiles and capacity when the initial state of energy (SOE) of ESDs were different. In [16], a novel dynamic programming based heuristic was proposed by jointly optimizing train speed profiles and regenerative energy. Although there have been many studies concerning the optimal train operation with ESDs, the attention is seldom concentrated upon the ones with on-board HESDs.

The suitable capacity for energy storage systems is becoming a hot topic both in the electric vehicle (EV) and electrified railway systems. A filtering based energy management strategy was reported, which aimed to minimize the weight and sizing of ESDs, and ensured the driving mission [17]. Likewise, an integrated optimization approach was also proposed to simultaneously achieve optimal sizing and weight of ESDs, where the wavelet-transform-based power management algorithm was employed [18]. Through in-depth analysis of the performance parameters of ESDs and DC/DC converters, an energy management framework was proposed to solve the sizing of BATs [19]. A study on the hierarchical energy management strategy was conducted to optimize the sizing of ESDs, where the system power profiles, the maximal power of SCs, and the capacity of BATs were considered [20]. The main focuses of these articles are only one or several driving cycles so that it is difficult to accurately evaluate the economic cost of ESDs after the long-term operation. On the other hand, the optimal sizing of ESDs or HESDs has

been considered with its role in train operations and many studies have been done to address the problem in the past. Kapetanović *et al.* [21] introduced sizing and energy management algorithms of Li-ion battery for railway vehicles, which aimed to minimize the fuel consumption and pollutant emission. Tang *et al.* [22] have studied the optimal sizing of HESDs based on an effective mutation particle swarm optimization method. By implementing a fixed-period energy management control for SCs and vanadium redox battery, the net present value of the optimal sizing of HESDs was fully evaluated. The optimal location and sizing of ESDs in DC electrified railway lines have been discussed in [23], [24], where the power flow of the train and the initial investment were considered. A techno-economic method was proposed to minimize the annual cost of the auxiliary battery-based substations, which could greatly define sizing, position, and control rules [25]. In [26], a novel MILP optimization model on the optimal sizing of stationary HESDs in electrified railway systems was presented, in which the cycles and depth of discharge of BATs were studied. To enhance power quality issues in railway systems, a sizing methodology based on a real-time simulation was proposed, which could accurately describe the relationship between capacity and power of ESDs [27]. Wu *et al.* [28] explored the problem of optimally sized ESDs installed in the trains, considering the constraints on capital cost and volume with an upper limit. In the above-mentioned papers, the optimal sizing of ESDs has been discussed, but the train speed trajectory optimization or the long-term train operation were not involved. For instance, only the economy of the short-term operation of the train was considered in [26], while the optimal sizing of ESDs was obtained under a fixed known train speed trajectory [28]. In summary, the optimal sizing problem based on collaborative optimization of the long-term train operation and on-board HESDs is worth a much deeper investigation to reflect the long-term perspective of train operation and whole-life cycle characteristics of HESDs.

Based on the above discussion, this paper focuses on the optimal sizing problem of on-board HESDs consisting of BATs and SCs and is concerned with the minimum cost which mainly includes the train's energy cost and the cost of the on-board HESDs arising from the initial investment and maintenance. Considering the long-term train operation, energy consumption and economic cost have become a hot topic both in the industrial and academic sector. In our previous work [14], [15], [29], it is found that the ESDs capacity will influence the optimal operation of the train, i.e., net energy consumption (NEC). Therefore, it will be interesting to consider the long-term train operation and study how the declining on-board HESDs capacity will affect train optimal operation and how to configure the capacity of the on-board HESDs to achieve the minimum cost. The contributions of this article are outlined as follows.

1) A mathematical model integrating the train speed trajectory and on-board HESDs composed of Li-ion battery and supercapacitor is proposed with detailed up-to-date
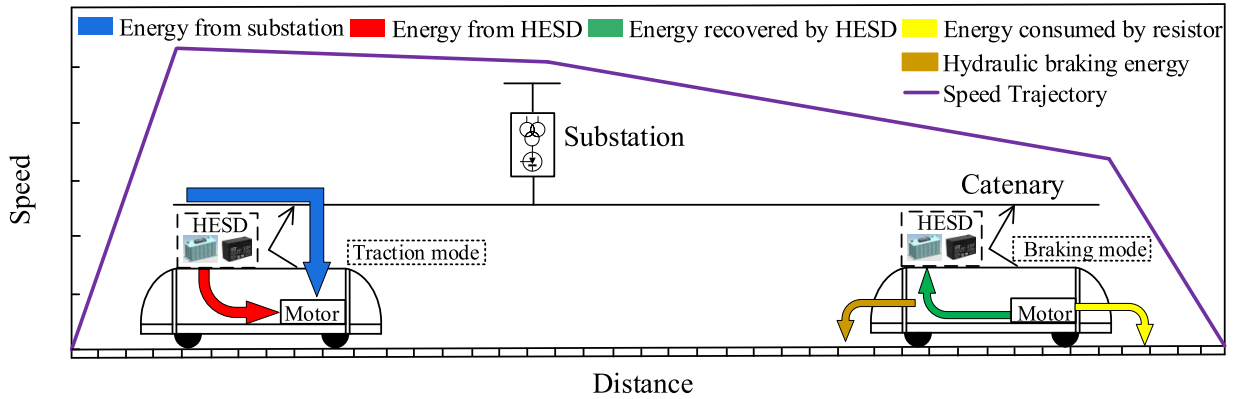
FIGURE 1. An illustrative diagram of speed trajectory and energy flow of train equipped with on-board HESDs.

engineering characteristics of HESDs including power density, energy density, and the total cycles throughout the entire lifetime.

2) An optimization framework for the long-term train operation and on-board HESDs sizing based on a developing state of health (SOH) degradation model is proposed. Combined with the long-term train operation, we revealed the economic performance and energy-saving rate of on-board HESDs with different investment ratios and allowable capital cost.

3) In practice, it is well known that the train speed trajectory can be changed dynamically, and it is highly coupled with the capacity of on-board HESDs. Compared with the existing literature, both the optimal train speed trajectory and the optimal sizing of on-board HESDs can be obtained by jointly modeling the train motion and the energy flow of on-board HESDs. The effectiveness of the proposed method can be further improved in the real-world train operation.

The remainder of this paper is organized as follows. Section II provides detailed information on the proposed model of the train operation, the energy flow modeling, the constraints, and the objective. In Section III, optimization results and discussion of different case studies are conducted. Finally, the conclusion and future work are presented in Section IV.

II. MODEL FORMULATION

In this section, the formulations of train movement and on-board HESDs energy flow based on the MILP approach are elaborated. As shown in Fig. 1, when the train is conducting traction operation, energy from the grid or on-board HESDs is distributed to the motors. Similarly, the energy generated by the train's regenerative braking operation can be recovered by on-board HESDs. Taking into account the constraints of on-board HESDs investment quota, the maximum power and capacity will be calculated and a proportion of the regenerative energy that can not be completely recovered by on-board HESDs will be consumed by the braking resistor.

A. A DISTANCE-BASED TRAIN OPERATION MODEL

The ith railway interstation length D_i is composed of several interval distances $\Delta d_{i,j}$ with different values. In the distance-based model, the train trajectory length D_i needs to be discretized and divided, which can be expressed by (1):

$$\sum_{j=1}^{N_i} \Delta d_{i,j} = D_i, \ i = 1, 2, 3 \ldots I \tag{1}$$

where N_i is the total number of the divided segments for D_i. Therefore, each interstation distance D_i has $(N_i + 1)$ speed points $V_{i,j}$, where $j = 1, 2, 3 \ldots N_i + 1$. In order to explore the effect of train speed trajectory in the long-term operation, the acceleration or deceleration value of the train is set to be unified in each interstation distance. It can be obtained as shown in (2):

$$a_{i,j} = \frac{\left(V_{i,j+1}^2 - V_{i,j}^2\right)}{2\Delta d_{i,j}} \tag{2}$$

where $a_{i,j}$ is the acceleration or deceleration for each $\Delta d_{i,j}$. In each $\Delta d_{i,j}$, the average speed $V_{i,j,ave}$ can be represented by (3):

$$V_{i,j,ave} = \frac{\Delta d_{i,j}}{\Delta t_{i,j}} = \frac{V_{i,j+1} + V_{i,j}}{2} \tag{3}$$

where $\Delta t_{i,j}$ is the interval time spent on each $\Delta d_{i,j}$. When the train is operating on the track, the drag force $F_{i,j,dr}$ can be expressed by the Davis Equation as shown in (4):

$$F_{i,j,dr} = A + BV_{i,j,ave} + CV_{i,j,ave}^2 \tag{4}$$

where A, B, and C are the Davis coefficients. During the journey, the maximum train speed must be limited due to real-world operation, and it can be set as shown in (5):

$$V_{i,j} \leq V_{i,j,\max} \tag{5}$$

where $V_{i,j,\max}$ is the speed limit constraints for each $\Delta d_{i,j}$. In the process of train motion optimization and modeling, the

journey time T_i of each interstation is also necessary to be constrained, as shown in (6):

$$\sum_{j=1}^{N_i} \Delta t_{i,j} \leq T_i, \; i = 1, 2, 3 \ldots I. \tag{6}$$

B. MODELING THE ENERGY TRANSMISSION OF TRAIN AND ON-BOARD HESDs

The energy flow is transmitted between the energy supply side (catenary or on-board HESDs) and the energy consumption side (train motor). In each $\Delta d_{i,j}$, when the train conducts traction or braking operation, it could either consume the energy from the substation and on-board HESDs or regenerate the energy then transfer it back to on-board HESDs. For each $\Delta d_{i,j}$, supposing $E_{i,j,t}$ is the traction energy and $E_{i,j,b}$ is the braking energy. During traction or cruising, the train motor consumes the energy from catenary $E_{i,j,c}$ with an efficiency η_{cat}, the energy discharged by the battery $E_{i,j,batd}$ with an efficiency η_{bat} and the energy discharged by the supercapacitor $E_{i,j,scd}$ with an efficiency η_{sc}. Thus, $E_{i,j,t}$ can be calculated by the following equation:

$$E_{i,j,t} = E_{i,j,c} \cdot \eta_{cat} + E_{i,j,b\ atd} \cdot \eta_{bat} + E_{i,j,s\ cd} \cdot \eta_{sc}. \tag{7}$$

The braking energy $E_{i,j,b}$ is considered to be equal to the sum of hydraulic braking energy $E_{i,j,hyd}$ and electric braking energy which might be recycled by on-board HESDs in each $\Delta d_{i,j}$. The energy $E_{i,j,batc}$ is transferred to the battery with an efficiency η_{bat} and the energy $E_{i,j,scc}$ is then transferred to the supercapacitor with an efficiency η_{sc}. The $E_{i,j,b}$ can be represented as follows:

$$E_{i,j,b} = -\left(\frac{E_{i,j,b\ atc}}{\eta_{bat}} + \frac{E_{i,j,s\ cc}}{\eta_{sc}} + E_{i,j,hyd} \right). \tag{8}$$

It is worth noting that considering the long-term train operation, η_{cat} is to specify the average transmission efficiency of energy from the substation to the train traction system. Similarly, η_{bat} and η_{sc} are to specify the average transmission efficiency of energy from the train traction system to on-board HESDs. Note that, when the train conducts regenerative braking, the $E_{i,j,b}$ is taken as a negative quantity. $E_{i,j,batc}$, $E_{i,j,scc}$ and $E_{i,j,hyd}$ are taken as positive quantities.

According to the energy conservation principle, when the train is in traction mode, $E_{i,j,t} \geq 0$, the electrical energy of the catenary and on-board HESDs is consumed by the motor and transformed into kinetic energy, potential, and heat energy. Similarly, when the train implements braking operation, $E_{i,j,b} \leq 0$, the kinetic energy is transformed into heat, potential energy, and electric energy that is fed back to on-board HESDs. Here, $E_{i,j,m}$ is the traction energy or the braking energy. The constraint of energy conversion could be expressed as follows:

$$E_{i,j,m} - \frac{1}{2} (M_t + M_{HESDs}) \left(V_{i,j}^2 - V_{i,j-1}^2 \right)$$
$$- F_{i,j,d\ r} \cdot \Delta d_{i,j} - (M_t + M_{HESDs}) g \Delta d_{i,j} \sin \theta_{i,j} \geq 0 \tag{9}$$

where the mass of the train, the mass of the on-board HESDs, and the gradient of the distance interval are denoted as M_t, M_{HESDs}, $\sin \theta_{i,j}$, respectively. Mathematically, the gradient of the distance interval $\sin \theta_{i,j}$ is related to the height difference of the distance interval $\Delta h_{i,j}$, namely $\Delta d_{i,j} \cdot \sin \theta_{i,j} = \Delta h_{i,j}$.

In addition to the energy conservation constraint, the power limit of train motors and on-board HESDs must be considered. Whether it conducts traction operation or braking operation, the actual power of the train can not exceed the maximum traction power $P_{t,\max}$ or the maximum braking power $P_{b,\max}$. Then it yields that

$$E_{i,j,c} \cdot \eta_{cat} + E_{i,j,b\ atd} \cdot \eta_{bat} + E_{i,j,s\ cd} \cdot \eta_{sc} \leq P_{t,max} \Delta t_{i,j} \tag{10}$$

$$\frac{E_{i,j,b\ atc}}{\eta_{bat}} + \frac{E_{i,j,s\ cc}}{\eta_{sc}} \leq P_{b,max} \Delta t_{i,j}. \tag{11}$$

For on-board HESDs, the charging and discharging power should not exceed the maximum power $P_{bat,\max}$, $P_{sc,\max}$ which holds that

$$E_{i,j,b\ atd} \leq P_{bat,max} \Delta t_{i,j}, \; E_{i,j,s\ cd} \leq P_{sc,max} \Delta t_{i,j} \tag{12}$$

$$E_{i,j,b\ atc} \leq P_{bat,max} \Delta t_{i,j}, \; E_{i,j,s\ cc} \leq P_{sc,max} \Delta t_{i,j}. \tag{13}$$

In the real operation of the train, the work done by the motor should be restricted by the maximum traction force $F_{t,\max}$ and the maximum braking force $F_{b,\max}$. Then it follows that

$$E_{i,j,c} \cdot \eta_{cat} + E_{i,j,b\ atd} \cdot \eta_{bat} + E_{i,j,sc\ d} \cdot \eta_{sc} \leq F_{t,max} \Delta d_{i,j} \tag{14}$$

$$\frac{E_{i,j,b\ atc}}{\eta_{bat}} + \frac{E_{i,j,s\ cc}}{\eta_{sc}} \leq F_{b,max} \Delta d_{i,j}. \tag{15}$$

The state of energy (SOE) is defined as the ratio of stored energy E_{stored} to the total capacity of on-board HESDs E_{cap} [30], which can be calculated in (16). Then (16) can be further written as (17) and accumulated after the train departs from the first station. It yields that:

$$SOE = \frac{E_{\text{stored}}}{E_{\text{cap}}} \times 100\% \tag{16}$$

$$\begin{cases} SOE_{i,j,bat} = \dfrac{E_{ini,bat} - \sum\limits_{j=1}^{N_i} E_{i,j,batd} + \sum\limits_{j=1}^{N_i} E_{i,j,batc}}{E_{cap,bat}} \times 100\% \\[4mm] SOE_{i,j,sc} = \dfrac{E_{ini,sc} - \sum\limits_{j=1}^{N_i} E_{i,j,scd} + \sum\limits_{j=1}^{N_i} E_{i,j,sc}}{E_{cap,sc}} \times 100\% \end{cases} \tag{17}$$

where $E_{ini,bat}$ and $E_{ini,sc}$ are the initial available capacity in the battery and supercapacitor, respectively. In this article, we aim to explore the energy-saving potential and economic of on-board HESDs over a wide range of SOE operating conditions, as well as avoiding full charge or full discharge. When the train departs and $j = 1, 2, 3 \ldots N_i$, the $SOE_{i,j}$ needs to be restricted during the journey, as shown in (18):

$$5\% \leq SOE_{i,j} \leq 95\%. \tag{18}$$

Then the total NEC value of the entire line can be expressed as follows:

$$\sum_{i=1}^{I} E_i = \sum_{i=1}^{I} \sum_{j=1}^{N_i} \sum_{l=1}^{L} (E_{i,j,c}^{l} + E_{i,j,b \ atd}^{l} + E_{ij,s \ cd}^{l} - E_{ij,b \ atc}^{l} - E_{i,j,s \ cc}^{l}) \quad (19)$$

where L is the total number of train operations. This is the primary objective function of the optimization model and the minimization of this function is to achieve the minimum energy from the catenary and maximize the remaining effective energy stored in the on-board HESDs.

In this study, battery and supercapacitor would have different lifetime cycles and state of health (SOH) considering the long-term train operation. With the increase of train mileage, the practical capacity and SOH of on-board HESDs will continue to degrade. The remaining lifetime cycles of the energy storage device are used to evaluate its SOH. In addition, a complete charging (e.g. $SOE_{i,j}$ from 0 to 100%) and discharging (e.g. $SOE_{i,j}$ from 100% to 0) operation is adopted to define as one lifetime cycle of the energy storage device. The SOH can be obtained by the ratio of the maximum practical capacity to the rated capacity. A similar method is adopted in [31]. SOH is calculated in (20):

$$\begin{cases} SOH_{i,j,b \ at}^{l} = \left(1 - \dfrac{\sum\limits_{l=1}^{L}\sum\limits_{j=1}^{N_i} E_{i,j,b \ atd}^{l} + \sum\limits_{l=1}^{L}\sum\limits_{j=1}^{N_i} E_{i,j,b \ atc}^{l}}{2 \times E_{cap,b \ at} \times LC_{bat}} \right) \\ SOH_{i,j,s \ c}^{l} = \left(1 - \dfrac{\sum\limits_{l=1}^{L}\sum\limits_{j=1}^{N_i} E_{i,j,s \ cd}^{l} + \sum\limits_{l=1}^{L}\sum\limits_{j=1}^{N_i} E_{i,j,s \ cc}^{l}}{2 \times E_{cap,s \ c} \times LC_{sc}} \right) \end{cases} \quad (20)$$

where LC_{bat} and LC_{sc} are the maximum lifetime cycles of battery and supercapacitor, respectively. Note that the actual capacity of $E_{cap,bat}$ and $E_{cap,sc}$ will decrease continually during the long-term operation. Thus, the initial energy of on-board HESDs satisfy the following constraint defined by (21):

$$\begin{cases} E_{ini,b \ at}^{l} = SOH_{i,j,b \ at}^{l-1} \cdot E_{cap,b \ at} \cdot SOE_{ini,b \ at} \\ E_{ini,s \ c}^{l} = SOH_{i,j,s \ c}^{l-1} \cdot E_{cap,s \ c} \cdot SOE_{ini,s \ c} \end{cases} \quad (21)$$

Traction and braking operations cannot be implemented simultaneously in reality, and this is reflected in the proposed model. Binary variables λ_i are introduced to ensure only one train operation mode is possible at each instance and it is realized in (22) as follows:

$$E_{i,j,m} = \lambda_i E_{i,j,t} - (1 - \lambda_i) E_{i,j,b} \quad (22)$$

where λ_i is equal to 0 or 1.

Moreover, the above variables should be restricted:

$$\begin{cases} 0 \le E_{i,j,c} \cdot \eta_{cat} \le \lambda_i M_1 \\ 0 \le E_{i,j,batd} \cdot \eta_{bat} \le \lambda_i M_1 \\ 0 \le E_{i,j,s \ cd} \cdot \eta_{sc} \le \lambda_i M_1 \\ 0 \le \dfrac{E_{i,j,batc}}{\eta_{bat}} \le (1 - \lambda_i) M_2 \\ 0 \le \dfrac{E_{i,j,s \ cc}}{\eta_{sc}} \le (1 - \lambda_i) M_2 \\ 0 \le E_{i,j,hyd} \le (1 - \lambda_i) M_2 \end{cases} \quad (23)$$

where M_1 and M_2 are two sufficiently large constants.

C. PIECEWISE LINEARIZATION USING SPECIAL ORDERED SET TYPE 2 (SOS2)

In this subsection, the piecewise linearization method in this paper is adopted to deal with nonlinear speed-related relationships, which need not transform the aforementioned basic motion equations. Furthermore, performing piecewise linearization of speed-related variables can increase the calculation speed and reduce the complexity of the model. The special ordered set type 2 (SOS2) contains a series of non-negative variables, and it is applied to piecewise linearization [32]. In SOS2, only two adjacent variables are greater than 0 and the sum of all variables is equal to 1. The relevant constraints are shown in (24)-(25):

$$\sum_{c=1}^{C} \alpha_{i,j}^{c} = 1 \quad (24)$$

$$0 \le \alpha_{i,j}^{c} \le 1, \quad c = 1, 2, 3 \ldots C \quad (25)$$

where $\alpha_{i,j}^{c}$ are variables of SOS2 in each $\Delta d_{i,j}$. The constant C is the number of the members in SOS2. To linearize the speed-related decision variables in (2), (3) and (4), $\delta_{i,j}$ is set to a small constant and denotes the linear part from $V_{i,j,\min}$ to $V_{i,j,\max}$, as shown in (26):

$$\delta_{i,j} = \frac{(V_{i,j,\max} - V_{i,j,\min})}{C} \quad (26)$$

where $V_{i,j,\min}$ and $V_{i,j,\max}$ are the minimum and maximum speed for each $\Delta d_{i,j}$, respectively. With the increase of C, the accuracy of the model will be improved, but the calculation time of the model will also be significantly longer. Then the decision variables $V_{i,j}$ and $V_{i,j}^2$ can be approximated as $V_{i,j}'$ and $V_{i,j}'^2$, respectively which can be calculated by using (27):

$$\begin{cases} V_{i,j} \approx V_{i,j}' = \sum_{c=1}^{C} (V_{i,j,\min} + (c-1)\delta_{i,j}) \cdot \alpha_{i,j}^{c} \\ V_{i,j}^2 \approx V_{i,j}'^2 = \sum_{c=1}^{C} (V_{i,j,\min} + (c-1)\delta_{i,j})^2 \cdot \alpha_{i,j}^{c} \end{cases} \quad (27)$$

Similarly, the decision variables related to average speed can be replaced by $V_{i,j,\ ave}'$, $V_{i,j,\ ave}'^2$ and $\frac{1}{V_{i,j,\ ave}'}$, respectively

which can be shown by (28):

$$
\begin{cases}
V_{i,j,\,\mathrm{ave}} \approx V'_{i,j,\,\mathrm{ave}} = \sum_{c=1}^{C} \left(V_{i,j,\min} + (c-1)\delta_{i,j} \right) \cdot \beta_{i,j}^{c} \\[2mm]
V_{i,j,\,\mathrm{ave}}^{2} \approx V'^{2}_{i,j,\,\mathrm{ave}} = \sum_{c=1}^{C} \left(V_{i,j,\min} + (c-1)\delta_{i,j} \right)^{2} \cdot \beta_{i,j}^{c} \\[2mm]
\dfrac{1}{V_{i,j,\,\mathrm{ave}}} \approx \dfrac{1}{V'_{i,j,\,\mathrm{ave}}} = \sum_{c=1}^{C} \dfrac{\beta_{i,j}^{c}}{V_{i,j,\min} + (c-1)\delta_{i,j}}
\end{cases}
$$
(28)

where $\beta_{i,j}^{c}$ are variables of another SOS2.

D. THE OBJECTIVE OF THE PROPOSED MILP MODEL

In summary, it can be seen from the above discussion that the objective of the proposed model is to minimize the value of the NEC, and on this basis, an economic evaluation of the full lifetime cycle of on-board HESDs must be conducted. Therefore, the degradation of on-board HESDs and NEC after the long-term train operation are expressed as economic costs C_{HESDs} and C_{NEC} for a unified evaluation of system performance. They are formulated in (29) and (30):

$$
\begin{aligned}
C_{NEC} = \sum_{i=1}^{I} \sum_{j=1}^{N_i} \sum_{l=1}^{L} & (E_{i,j,c}^{l} + E_{i,j,batd}^{l} + E_{ij,scd}^{l} \\
& - E_{i,j,batc}^{l} - E_{i,j,scc}^{l}) \cdot \mathrm{Pr}_1
\end{aligned}
$$
(29)

$$
\begin{aligned}
C_{HESDs} = & \left(1 - SOH_{i,j,b\ at}^{l} \right) \cdot E_{cap,b\ at} \cdot \mathrm{Pr}_{bat} \\
& + \left(1 - SOH_{i,j,s\ c}^{l} \right) \cdot E_{cap,s\ c} \cdot \mathrm{Pr}_{sc}
\end{aligned}
$$
(30)

where Pr_1, Pr_{bat}, and Pr_{sc} are the price of electricity, battery, and supercapacitor in \$/kWh, \$/MJ, and \$/MJ, respectively. Furthermore, the extra cost of on-board HESDs C_{HESDs}^{E} needs to be considered, including installation and maintenance, which is positively related to the respective initial capacity of energy storage equipment.

$$
C_{HESDs}^{E} = \omega_1 \cdot E_{cqp,b\ at} \cdot \mathrm{Pr}_{bat} + \omega_2 \cdot E_{cap,s\ c} \cdot \mathrm{Pr}_{sc}
$$
(31)

where ω_1 and ω_2 are fixed constant coefficients. The proposed MILP model aims to coordinate optimization to minimize the total economic cost of railway vehicles and on-board HESDs. Then the optimization is given as shown in (32):

$$
\begin{aligned}
&Min \quad C_{NEC} + C_{HESDs} \\
&\text{Subject to:} \quad (1)-(30)
\end{aligned}
$$
(32)

The proposed model can efficiently determine the optimal sizing configuration of on-board HESDs, after considering the tradeoff between energy-saving rate and the economics of the whole lifetime cycle of on-board HESDs.

III. CASE STUDIES AND RESULT DISCUSSION

In this section, many cases for multiple on-board HESDs configuration scenarios are discussed by using a real project based on the data from the Beijing Changping line such as
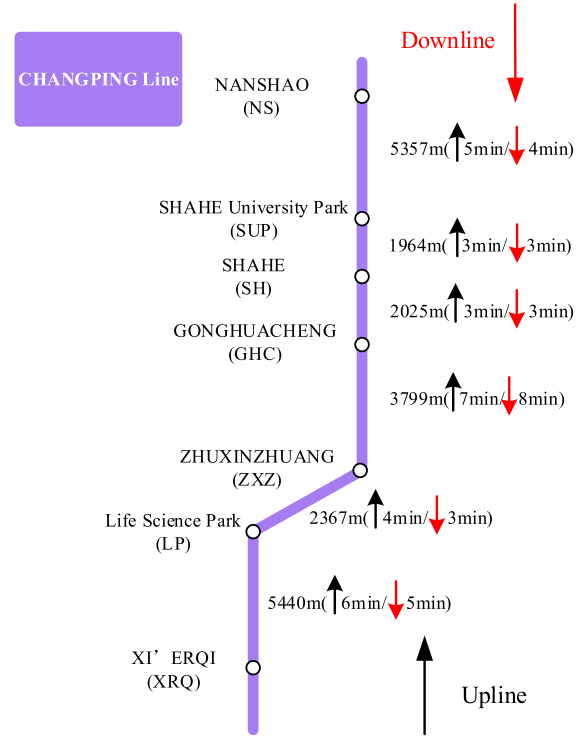

FIGURE 2. The station information map of the Beijing Changping Line.

mass, gradient, and distance, etc. The Changping line covers a distance of 20952 m and has seven stations, whose route map is shown in Fig. 2. Three scenarios corresponding to subsection A, B, and C in the case studies are conducted as follows:

- All cases including the investment ratio of Li-ion battery is greater than, equal to, and less than that of supercapacitor are listed with the upper limit of the capital cost being 20 k\$. Here for the sake of compactness, only one case is selected and the operation of the train running at interstation and the whole Changping line are displayed and analyzed to verify the rationality and correctness of the model.
- Considering the degradation of on-board HESDs caused by the long-term train operation, the changing trends of SOH and NEC under different configuration ratios on-board HESDs have been further investigated.
- As a comparison, single or both of the ESDs in on-board HESDs are no longer in effective status after the long-term train operation. Based on the results of the above-mentioned cases, the comparison and analysis of the economy and energy-saving effect are given.

The parameters in the Changping line have been tabulated in Table 1. The mass of the train in the Changping line is 199 tons without on-board HESDs, and the maximum traction and regenerative braking force are set to be the same [28], [33]. The maximum acceleration a_a and deceleration a_d are both set to be the same and this applies to both maximum traction and braking power. As for the average energy

TABLE 1. Key parameters in the Changping Line for a typical railway vehicle with on-board HESDs.

Symbol	Description	Value
$M_t(\text{t})$	Total mass of the train	199
$P_{t,m}(\text{kW})$	Maximum traction power	3700
$P_{b,m}(\text{kW})$	Maximum braking power	3700
$a_{a,max}(\text{m/s}^2)$	Maximum acceleration	1.0
$a_{b,max}(\text{m/s}^2)$	Maximum deceleration	1.0
$D(\text{m})$	Total travel distance	41904
$\eta_bat(\%)$	Li-ion Battery efficiency	0.9
$\eta_{sc}(\%)$	Supercapacitor efficiency	0.9
$\eta_cat(\%)$	Motor efficiency	0.8
$\Delta d(m)$	Distance interval	100
$F_{t,max}(\text{kN})$	Maximum traction effort	310
$F_{b,max}(\text{kN})$	Maximum braking effort	310
$A(\text{kN})$	Davis coefficient	2.0895
$B(\frac{\text{kN}}{\text{m/s}})$	Davis coefficient	0.0098
$C(\frac{\text{kN}}{\text{m}^2/\text{s}^2})$	Davis coefficient	0.0065

efficiency of on-board HESDs η_{bat} and η_{sc}, we set them to be 0.9 considering negligible transmission loss [15], [29]. Similarly, we consider that there will be an average loss of 10% when the energy is transmitted from the grid to the train motor via the catenary. As far as we know, the highest efficiency of the state-of-the-art electric train does not exceed 0.97, and then it is approximately set to be 0.9 [10]. Considering the transmission loss and motor efficiency, the value of η_{cat} is approximately set to be $0.8 \approx 0.9 \times 0.9$. The distance interval Δd is set to be 100 m, which can be modified in real train operation optimization.

In addition, the main parameters for on-board HESDs are shown in Table 2, which have been verified by referring to the literature [1], [34]. For the sake of generality of the model parameters, we have chosen the arithmetic mean of the capacity cost, energy density, power density and lifetime of on-board HESDs in Table 2 as model simulation parameters, e.g., the capacity cost for Li-ion battery is set to be $(500 + 2500)/2 = 1500$ \$/kWh and supercapacitor is set to be $(2000 + 10000)/2 = 6000$ \$/kWh. The arithmetic mean is considered to reflect the general characteristics of various data sets of on-board HESDs.

Note that case studies are conducted by using PYTHON 3.7.2 and GUROBI 9.1.1 solver on a PC with Intel Core i7-9700 processor (3.60GHz) and 16-GB RAM.

A. STUDIES ON THE OPERATION OF THE TRAIN WITH ON-BOARD HESDs

In this subsection, the case studies are aimed at exploring how different investment configuration ratios of the on-board HESDs influence the train speed trajectory, NEC, and energy flow to verify the reliability of the model. Notice that, in general, the investment configuration ratios of the on-board HESDs could be considered as an optimization variable. However, it is regarded as a known parameter to keep the model linear and reduce the computational complexity. A similar approach is applied in [26]. The different investment configuration ratios of on-board HESDs and

corresponding resulted capacity, maximum power, and mass are listed in Table 3. It is also worth pointing out that, as a comparison, the solutions of ''Li-ion battery only'' and ''supercapacitor only'' are listed in case 6 and case 13, respectively. It indicates that that with the increase of Li-ion battery investment configuration ratios, the maximum power and mass appear a downward trend.

As shown in Figs. 3 and 4, the optimal operation of the train is displayed when the train runs at the interstation (between XRQ and LP) and the entire Changping line. Here for the sake of compactness, only the operation of the train for case 1 is demonstrated and analyzed to verify the correctness of the model, which can be modified according to practical conditions.

In Fig. 3, it is shown that when the distance is from 0 m to 400 m, the traction energy of the train mainly comes from the catenary and discharge energy by on-board HESDs. Subsequently, the potential energy of the train caused by height difference can be converted into kinetic energy, on-board HESDs energy, and heat energy. During braking operation, kinetic energy can be converted into electrical energy which can be recovered by the on-board HESDs. It can be observed that the Li-ion battery can not only be discharged during the acceleration of the train but also can be charged, which indicates that the train needs to accelerate slowly under the slope limit to meet the journey distance and time constraints. On the other hand, the Li-ion battery is not only allowed to be charged during the deceleration of the train but can also be discharged to support the climbing the slope operation of the train. It is worth mentioning that the train operation conforms to the law of conservation of energy, and when the power is less than 0, it means that the on-board HESDs are in the charging state.

Similarly, it is found that the optimal operation of the train running on the Changping upline and downline for case 1 are shown in Fig. 4. It should be noticed that the operation of Changping upline and downline would be regarded as a complete optimization process. In Fig. 4(a) and 4(b), the detailed on-board HESDs power and SOE profiles for case 1 are presented and it is evident that the charge/discharge speed of the supercapacitor is faster than that of the Li-ion battery due to their respective property. When the initial SOE in on-board HESDs are different during the optimization process, the charging and discharging strategy of on-board HESDs may result in different train operation modes [15], [35]. Therefore, the initial $SOE_{ini,bat}$, and $SOE_{ini,sc}$ are uniformly set to be 0.5, and they can also be modified to any value according to the field data. As shown in Fig. 3 and Fig. 4, detailed operation of the train is demonstrated which runs for the first time, namely SOH = 100%. In order to elaborate on how different investment configuration ratios of the on-board HESDs influence the optimal operation of the train, the operation results are listed in Table 4.

In Table 4, it is shown that when the railway vehicle operations with constant on-board HESDs investment configuration ratio such as case1 for the long-term train operation,

TABLE 2. Technical characteristics of on-board HESDs [1], [34].

On-board HESDs type	Energy density (kWh/t)	Power density (kW/t)	Capacity cost ($/kWh)	Lifetime (cycles)
Li-ion battery	75-200	100-350	500-2500	1000-3000
Supercapacitor	2.5-15	500-5000	2000-10000	60000-100000

TABLE 3. Parameters of on-board HESDs investment configuration ratio, maximum power, mass, capacity with an upper limit of capital of 20 k$.

| Case	Investment ratio (Li-ion Battery:Supercapacitor)	Li-ion battery maximal power (kW)	Supercapacitor maximal power (kW)	Total capacity (MJ)	Mass (kg)
1	2:1	14.5	349.2	36	202.1
2	3:1	16.3	261.9	39	175.4
3	4:1	17.4	209.5	40.8	159.4
4	5:1	18.2	174.6	42	148.7
5	10:1	19.8	95.2	44.7	124.4
6	1:0	21.8	0	48	95.3
7	1:1	10.9	523.8	30	255.5
8	1:2	7.27	698.4	24	309.0
9	1:3	5.45	785.7	21	335.6
10	1:4	4.36	838.1	19.2	351.6
11	1:5	3.63	873	18	362.3
12	1:10	1.98	952.3	15.3	386.6
13	0:1	0	1047.7	12	415.7
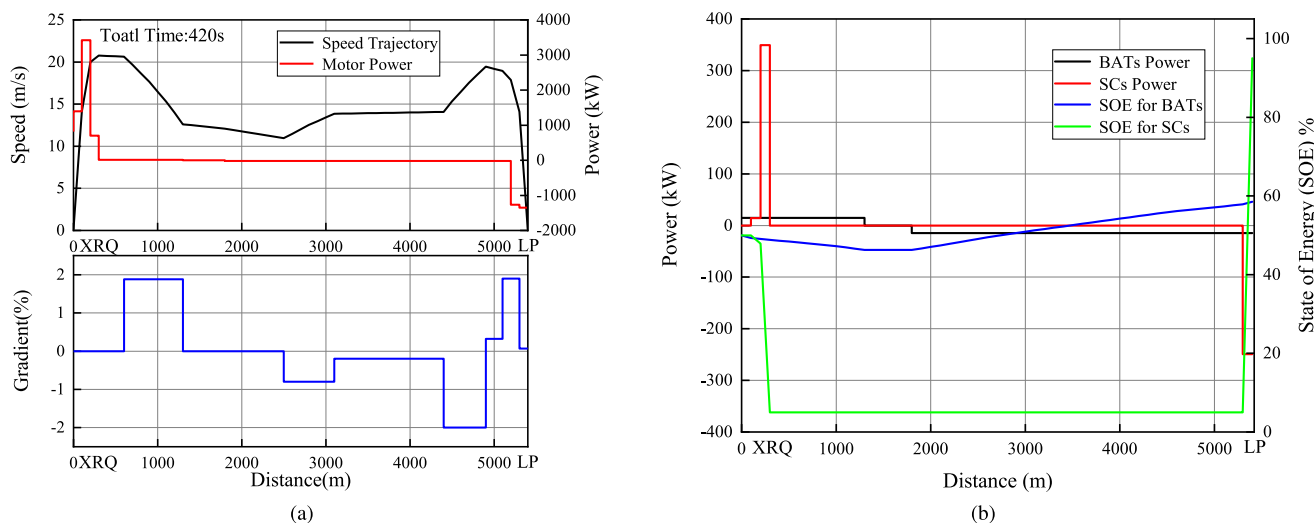
FIGURE 3. The optimal operation of the train running on the interstation journey (from XRQ to LP) for case 1.(a) The train speed trajectory, gradient information, and motor power. (b) The discharge/charge power and SOE curves.

the total discharge/charge energy could continue to decrease, but the value of NEC continuously increases slightly which is from 374.37 MJ to 377.47 MJ. It means that with the reduction of on-board HESDs remaining capacity and rechargeable energy, the railway vehicle is unable to recover more regenerative braking energy, which results in the on-board HESDs would gradually lose energy-saving potential after the long-term train operation [15].

On the contrary, it is easily noted that the value of NEC for 1st running see first decrease continuously and then rise slightly when the investment proportion of supercapacitor keeps increasing. It means that even though on-board HESDs are provided with higher power, railway vehicles cannot absorb more electrical energy converted from kinetic energy to achieve energy-saving operation.

B. STUDY ON NEC AND SOH FROM A LONG-TERM PERSPECTIVE

The influence of the on-board HESDs with different investment configuration ratios on the changing trend of NEC and SOH is investigated in this subsection. The life cycles of Li-ion battery and supercapacitor are set to be 2000 and 80000 times, respectively, according to the data in Table 2. The relationship between the SOH and operation times for cases 1-5 is shown in Fig. 5, in which the investment proportion of Li-ion battery is larger than that of supercapacitor. Note that, a complete operation means that the train has accomplished the Changping upline and downline. It can be found that with the increase of operation times, the SOH of the Li-ion battery in case 1 is the best, about 21.1%, and the SOH of the Li-ion battery in case 5 is the worst, about 18.4%.
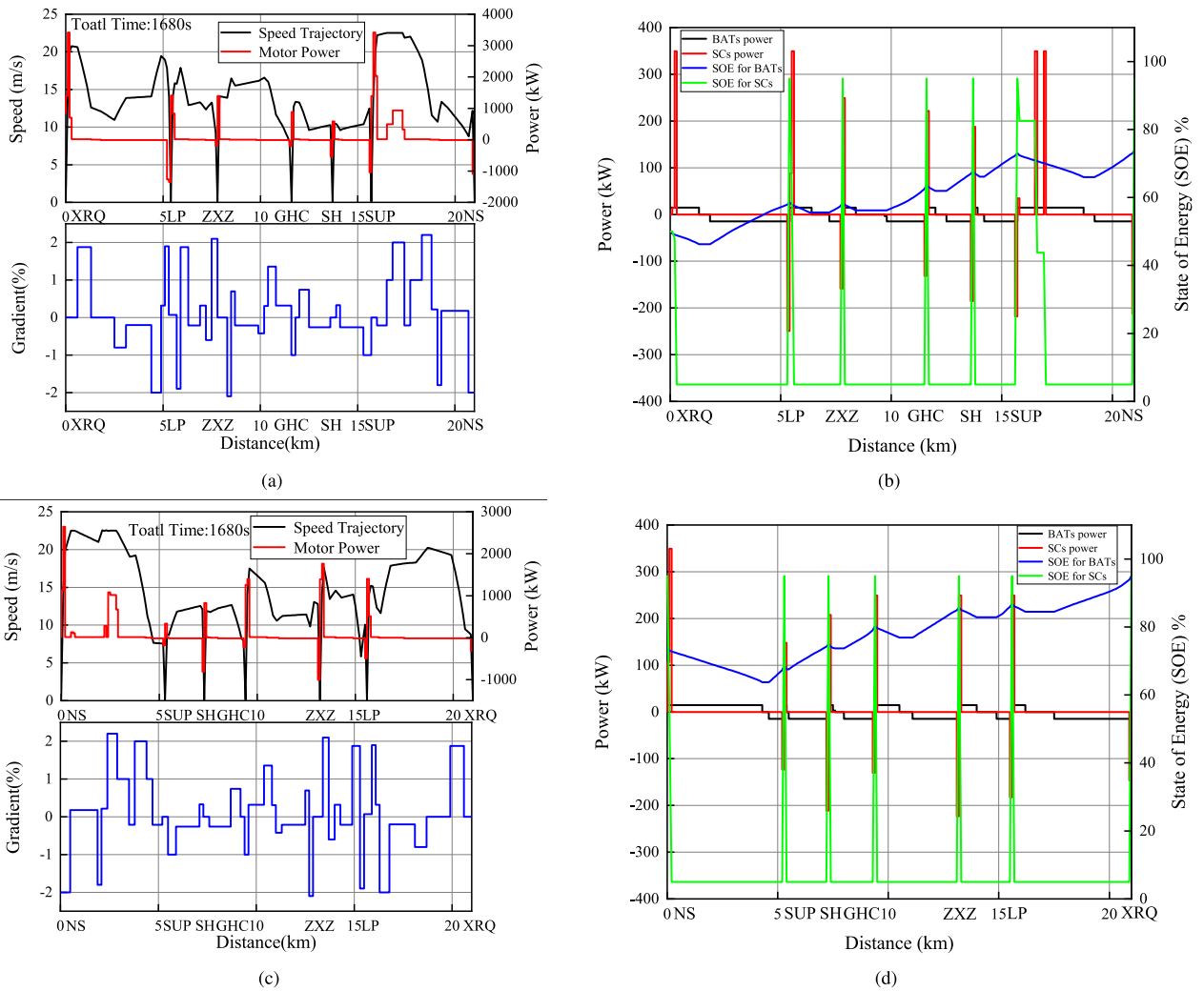
FIGURE 4. The optimal operation of the train on the Changping upline and downline for case 1.(a) The train speed trajectory, gradient information, and motor power for the Changping upline operation. (b) The discharge/charge power and SOE curves for the Changping upline operation. (c) The train speed trajectory, gradient information, and motor power for the Changping downline operation. (d) The discharge/charge power and SOE curves for the Changping downline operation.

TABLE 4. The operation results of the changping upline and downline for cases 1-13.

Case	Number of running	Energy from catenary (MJ)	Total discharge/charge energy (MJ)	NEC(MJ)	Investment ratio(Li-ion Battery:Supercapacitor)
	1st	390.57	54.35/70.55	374.37	
	100th	390.69	54.27/69.93	374.97	
1	200th	390.80	54.11/69.32	375.59	2:1
	300th	390.90	53.72/68.40	376.22	
	400th	391.00	53.31/67.47	376.84	
	500th	391.10	53.06/66.69	377.47	
2	1st	401.75	45.78/63.33	384.20	3:1
3	1st	408.51	42.51/60.87	390.15	4:1
4	1st	413.01	37.08/55.98	394.11	5:1
5	1st	423.31	29.32/49.44	403.19	10:1
6	1st	437.13	19.14/41.91	414.36	1:0
7	1st	368.12	72.10/85.22	355.00	1:1
8	1st	346.51	89.63/99.54	336.60	1:2
9	1st	322.36	114.11/119.66	316.81	1:3
10	1st	328.22	107.07/113.42	321.87	1:4
11	1st	331.28	103.73/110.65	324.36	1:5
12	1st	336.84	98.34/106.46	328.72	1:10
13	1st	369.15	62.09/64.79	366.45	0:1

This indicates that in the cases with larger capacity and higher power of Li-ion battery, especially case 5, the optimization model will choose to apply the Li-ion battery to be frequently charged and discharged. Therefore, the Li-ion battery in case 5 degrades faster than that in other cases. In addition, it can be observed that when the SOH reaches
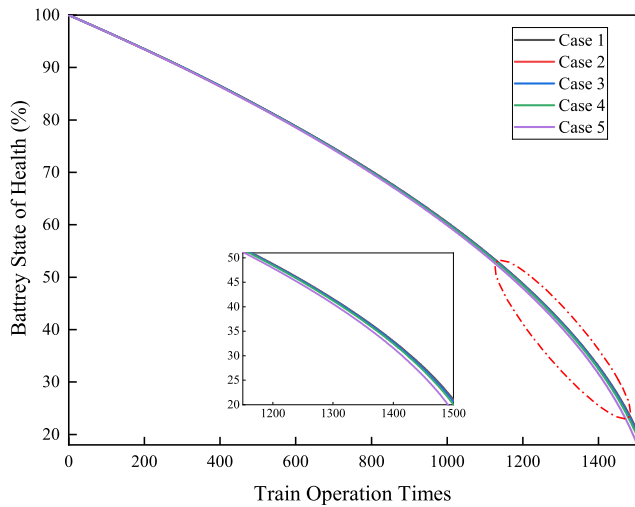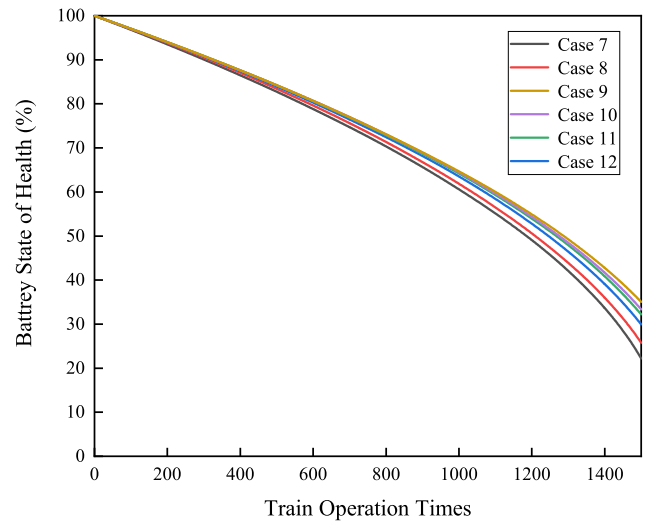
FIGURE 5. Relationship between the SOH and operation times for different sized on-board HESDs.

about 64%, the degradation rate of the Li-ion battery starts to increase.

When the investment proportion of supercapacitor is larger than or equal to that of Li-ion battery, the relationship between the SOH and operation times for cases 7-12 is plotted in Fig. 6. In Fig. 6, it can be found that the SOH of Li-ion battery and supercapacitor see an interesting trend for cases 7-12, in which they seem to first rise and then fall. The SOH value of on-board HESDs is the highest in case 9, which are 35.8% and 81.2%, respectively, and the lowest in case 7, which are 22.2% and 80.1%, respectively. When the SOH of the Li-ion battery reaches about 85%, the battery in cases 7-12 obviously exhibits different rates of deterioration. However, the results for supercapacitors show an almost linear decline in cases 1-5 and cases 7-12. It is worth mentioning that the decay process of the supercapacitor in cases 1-5 and cases 7-8 is completely the same, which may be related to its large number of cycles. On the other hand, it is implied that the supercapacitor in cases 1-5 and cases 7-8 has realized the same strategy of discharge and charge when the train runs each interstation in the whole Changping line.

From the abovementioned case studies, the relationship between the value of NEC and different optimally sized on-board HESDs under varying train operation times are illustrated in Fig. 7. It can be noted from Fig. 7 that with the increase of train operation times and the investment proportion of Li-ion battery in the on-board HESDs, the NEC increases continually in cases 1-5 which is plotted in the range of the axis 0:1 to 1:1. On the other hand, it can be seen that with the increase of train operation times and the investment proportion of supercapacitor in the on-board HESDs, there is an interesting trend in the value of NEC in cases 7-12, namely to first drops quickly and then rises slightly. It can be clearly observed that the minimum net energy consumption can be obtained when the investment ratio of the supercapacitor to Li-ion battery is 3:1.

(a)
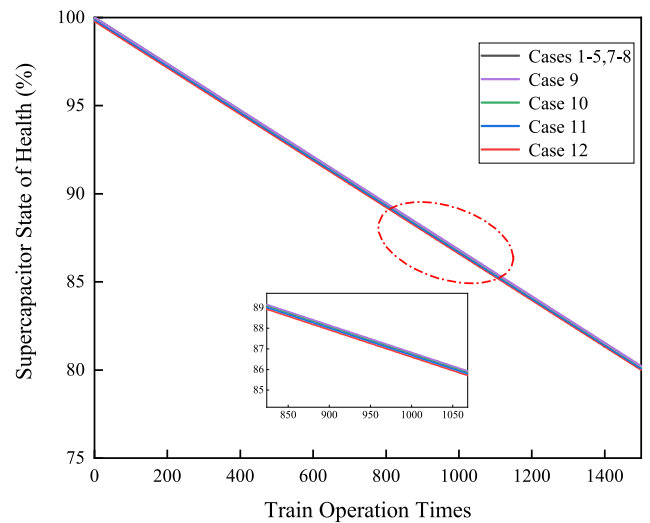
(b)

FIGURE 6. Relationship between the SOH and operation times. (a) SOH change of Li-ion battery. (b) SOH change of supercapacitor.

The NEC under varying train operation times is illustrated in Fig. 8, which is the projected plane of Fig. 7 from the inside. In terms of the changing trends of NEC, the performance of case 3 is close to that of case 4, and case 5 might be deprived of its energy-saving potential due to improper configuration ratio of on-board HESDs in Fig. 8(a). In Fig. 8(b), from the perspective of the energy-saving effect, the performance of Cases 9-11 is very close when the number of operations is less than 200. Compare with previous case studies such as cases 1-5, the NEC in cases 7-12 is generally lower than that in cases 1-5, which is also in line with the fact that the energy-saving rate of the supercapacitor is higher than that of Li-ion battery [5]. However, it can not be ignored that continuously increasing the investment ratio of supercapacitor in on-board HESDs will not cause lower NEC, which may be because the supercapacitor with higher investment ratio will reduce the rechargeable capacity of on-board HESDs.
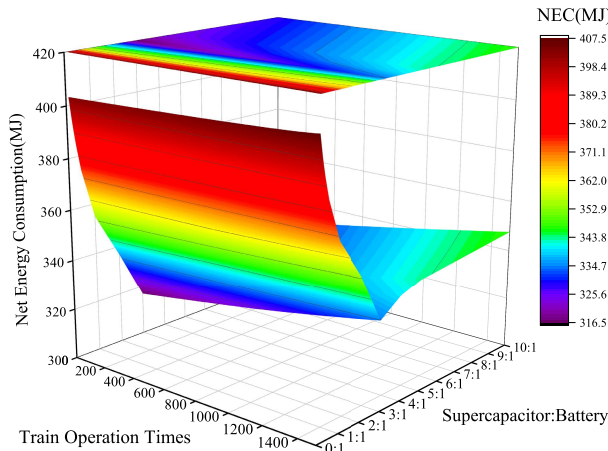
FIGURE 7. The NEC for different sized on-board HESDs under varying train operation times.

C. COMPARATIVE STUDIES ON ECONOMIC AND ENERGY-SAVING PERFORMANCE

The sizing of on-board HESDs favored the economic index by achieving the minimization of the total costs of the train and on-board HESDs. Considering the long-term train operation, the electricity bills generated by the NEC, and the costs by on-board HESDs degradation and maintenance are important sources of total costs and directly affect economic evaluation.

In this subsection, the comparison and analysis of the economy and energy-saving performance for the proposed model is elaborated based on the results of all the abovementioned cases.

For this scenario, after the railway vehicle conduct the long-term operation, a single or both of the ESDs in on-board HESDs may be no longer in effective status due to the significant difference in their respective life cycles. Therefore, as a comparison, it is necessary to verify the cases of single or no ESDs in the train from the perspective of economical and energy-saving.

The analysis of the economy mainly takes into account the following factors and criteria:

- The degradation cost of the on-board HESDs C_{HESDs} is related to the current respective SOH value. For instance, when the SOH value of the Li-ion battery is 70%, the degradation cost it generates is 30% of the total investment in the Li-ion battery.
- In the optimization process, since the cases of "Li-ion battery only" and "supercapacitor only" need to be investigated and compared and their investment ratios are dynamically changing in different case studies, so we consider that the operation times should be unified, i.e. 1500 times corresponding to 62856 km, which is the total mileage of the train for one and a half months and can be modified according to the case studies.
- Considering the current industrial user electricity energy prices in China, it was evaluated considering a value
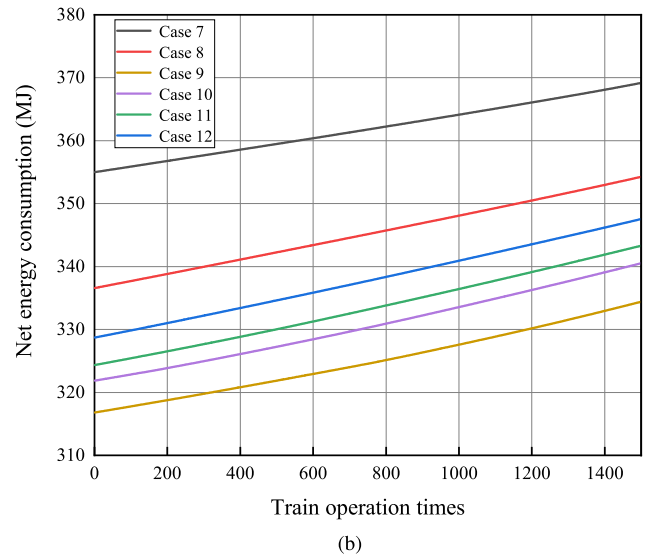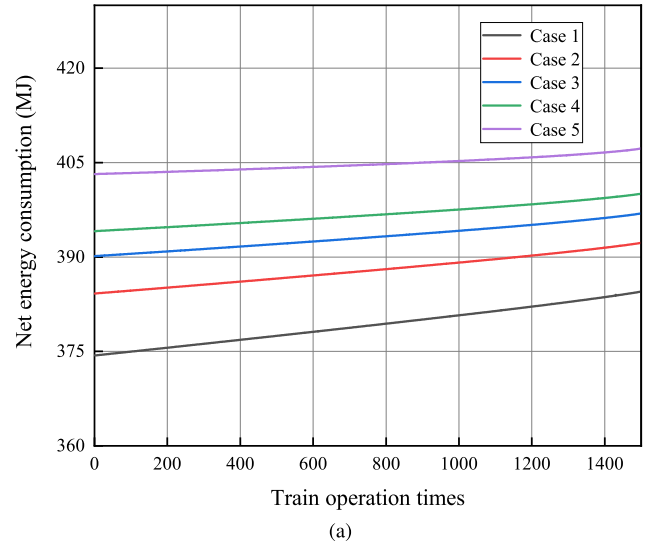

FIGURE 8. The NEC for different sized on-board HESDs. (a) The NEC results for Cases 1-5. (b) The NEC results for cases 7-12.

of 0.16 USD/kWh during the time period of peak load (8:00-12:00 and 17:00-21:00) [36].

- More in detail, the on-board HESDs need to consider extra costs in terms of installation and maintenance. About Li-ion battery, the extra cost of it is 300,000 \$/MWh, which is a common parameter and used in [26], [37]. Then the ω_1 in (31) is set to be 0.2, which mainly includes the extra cost of BMS and battery packaging. About the supercapacitor, the extra cost of it is 7976 \$/MW, which is a common parameter and used in [38], [39]. Then the ω_2 in (31) is set to be 0.4, which has mainly been considered including the extra cost of assembling the stack.

Similarly, the following energy-saving criteria have been chosen:

- When the railway vehicle operates without the on-board HESDs, the value of NEC is 436.73 MJ. It is noted

TABLE 5. The cost/energy-saving rate analysis for the above cases.

| Case	Average NEC(MJ)	Energy-saving rate (%)	C_{NEC} ($)	C_{HESDs} ($)	C_{HESDs}^{E} ($)
1	379.18	13.18	25279	11846	5333
2	387.93	11.17	25862	12887	5000
3	393.21	9.97	26214	13490	4800
4	396.74	9.16	26450	13984	4667
5	404.80	7.31	26987	15181	4364
6	414.75	5.03	27658	16502	4000
7	361.87	17.14	24125	9767	6000
8	345.23	20.95	23016	7594	6667
9	324.95	25.59	21663	6030	7000
10	330.6	24.30	22040	5853	7200
11	333.39	23.66	22226	5586	7333
12	337.87	22.63	22525	5226	7636
13	373.30	14.52	24887	4420	8000
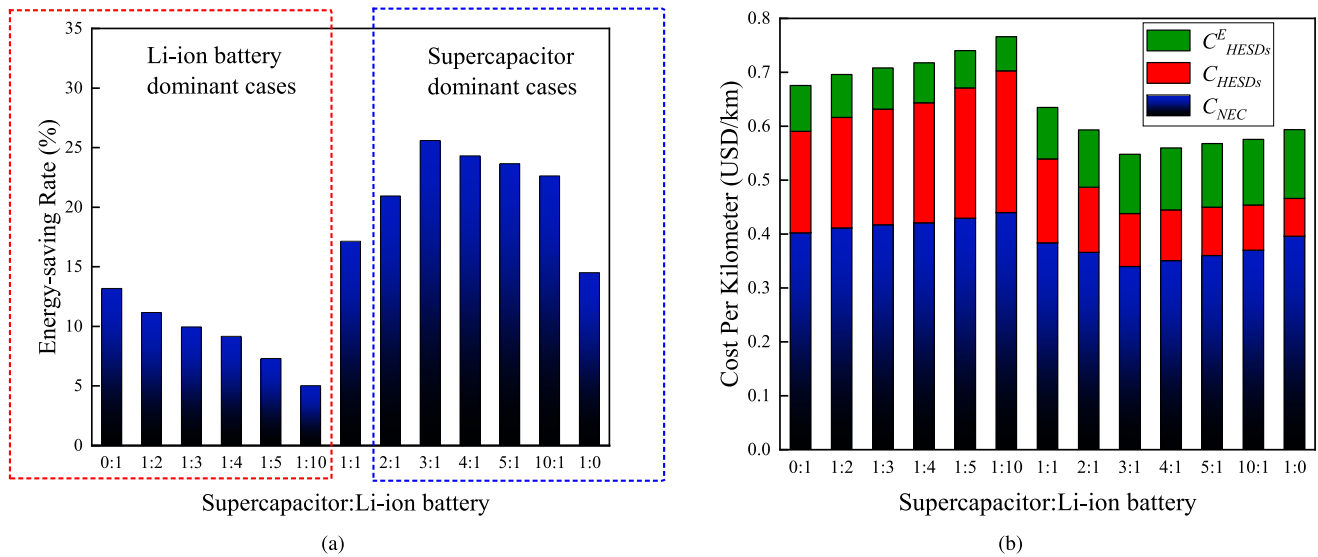
FIGURE 9. The energy-saving rate and economic cost versus the different investment ratio of on-board HESDs for all cases. (a) Average energy-saving rate for all cases. The Li-ion battery with higher investment ratio in cases 1-6, the energy-saving rate is lower, while the energy-saving rate first rises and then drops in the cases 7-13 with higher supercapacitor. (b) Components of cost per kilometer for all cases. The Li-ion battery with higher investment ratio in cases 1-6, the cost per kilometer is higher, while the cost per kilometer first drops and then rises in the cases 7-13 with higher supercapacitors.

that the energy-saving rate of all cases are calculated in reference to the scenario without on-board HESDs.

- Considering that the NEC of all cases change dynamically during the long-term train operation, we choose the average NEC of each journey to evaluate the energy-saving rate.

The main objective of the above analysis was related to the identification of the energy-saving rate and economic cost. Results of all cases are detailed in Table 5.

Based on the above results, the energy-saving rate and cost per kilometer are used to evaluate the optimal sizing of on-board HESDs, which is plotted in Fig. 9. It is worth mentioning that the economic cost is determined based on the following three parts.

1) C_{NEC}: The electricity cost generated by the NEC of the train.
2) C_{HESDs}: The cost generated by the degradation of on-board HESDs.

3) C_{HESDs}^{E}: The extra cost of on-board HESDs needs to be considered, including installation and maintenance.

Fig. 9 shows the trend of the energy-saving rate and economic cost versus the different investment ratio of on-board HESDs. As visible, when the investment proportion of Li-ion battery is greater than that of the supercapacitor in cases 1-6, the energy-saving rate continues to decline, and the cost per kilometer increases significantly with the increase of the investment proportion of Li-ion battery. Similarly, it can be observed that with the increase in the investment proportion of supercapacitor, the energy-saving rate first rises and then declines slightly, whereas the cost per kilometer is just the opposite in cases 7-13. It must in fact be said that the lowest energy-saving rate in case 6 is 5.03% and the highest cost per kilometer is 0.76 USD/km, while the highest energy-saving rate in case 9 is 25.59% and the lowest cost per kilometer is 0.55 USD/km. Obviously, the minor energy-saving rate is not conducive to the long-term train operation, because the
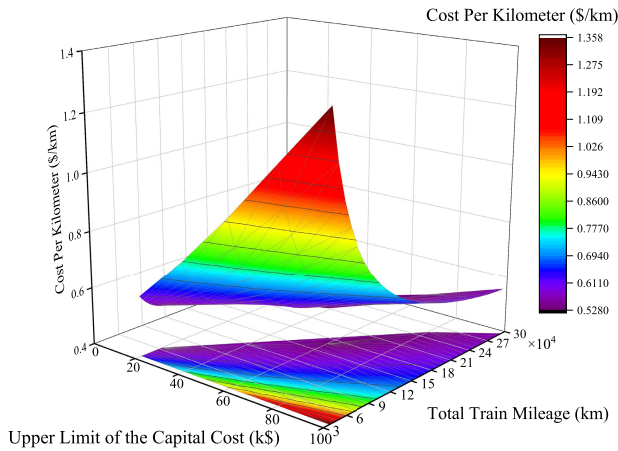
FIGURE 10. The cost per kilometer for on-board HESDs under varying capital cost limit and total train mileage.
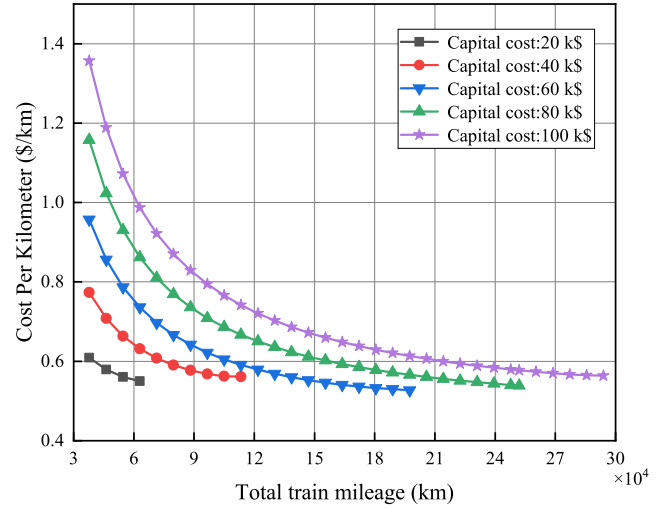

FIGURE 11. Different change trends for cost per kilometer of on-board HESDs with respect to the upper limit of the capital investment and total train mileage.

electricity bill generated by it accounts for a higher proportion of the total economic cost, which leads to expensive cost per kilometer.

It should be mentioned that the Li-ion battery known for its energy density will bring more rechargeable capacity to on-board HESDs, while the supercapacitor known for its power density will enable on-board HESDs to be discharged or charged more quickly during traction or braking operation of train. It means that the optimization problem was to explore tradeoffs between the investment ratio of Li-ion battery and that of supercapacitor with the upper limit of the capital cost being 20 k$. Based on the abovementioned results, it can be seen that when the investment ratio of the supercapacitor to Li-ion battery is 3:1, the optimization model obtains the optimal solution. This also further illustrate that the on-board HESDs with the appropriate configuration ratio can indeed optimize the energy-saving rate and economic cost, considering the long-term train operation. In addition, although the solution of "supercapacitor only" can bring a better economic performance in the degradation cost of ESDs, the lower energy-saving rate leads to the higher overall economic cost.

Based on the above optimization results, Fig. 10 depicts further on the relationship between capital investment and total train running mileage and cost per kilometer, which helps us to investigate the economic performance of the electric trains under variable capital investment after the long-term operation. When the initial capital investment of on-board HESDs is relaxed to be higher, it means that electric trains with higher capital investment of on-board HESDs will travel longer distances. Therefore, a constant SOH value of on-board HESDs should be set during the optimization process, instead of the operation times. We consider that when the SOH value of on-board HESDs reaches 35%, the model stops the optimization process, and it can be modified according to real engineering applications. In Fig. 10, the range of capital investment is from 20 k$ to 100 k$ with an increment

step of 10 k$, and the range of total train mileage is 30,000 km to 300,000 km with an increment step of 30,000 km, which can improve the applicability of the model in real engineering applications. From Fig. 10, it is worth noting that the cost per kilometer continues to drop when the total train mileage increases. It means that the extra cost of on-board HESDs would undermine the economic index when the total train mileage is relatively low. The changing trend for cost per kilometer of on-board HESDs with respect to the capital investment and the total train mileage is illustrated in Fig. 11, which is a projected plane of Fig. 10. It can be observed that when the capital investment is relaxed from 20 k$ to 60 k$, the cost per kilometer drops from 0.55 USD/km to 0.53 USD/km. When the capital investment was allowed to continue to go higher, the cost per kilometer rise from 0.53 USD/km to 0.56 USD/km. It is implied that although the capital investment quota has been relaxed to be higher than 60 k$, the on-board HESDs with higher capacity and power cannot significantly improve the energy-saving rate in the long-term train operation so that the cost per kilometer continues to increase. The result provides a clear guidance on how to select the appropriate proportion of on-board HESDs considering the long-term train operation.

IV. CONCLUSION AND FUTURE WORK

In this paper, a MILP model for the optimal sizing of on-board HESDs composed of Li-ion battery and supercapacitor has been developed in electric railway systems. The main attractiveness of the proposed model resides in the combination of the long-term train operation together with the sizing problem of emerging on-board HESDs. The goal of the proposed model is to minimize the total economic cost caused by the long-term train operation and the degradation and maintenance of on-board HESDs for practical engineering applications, which are the key factors concerned by railway energy

systems planners and operators. We have modeled in detail the operation of the train and the energy flow of on-board HESDs in a real-world case of the Beijing Changping line. More specifically, we have demonstrated that the capacity and power of on-board HESDs can be dynamically modified by changing the configuration ratio of Li-ion battery or supercapacitor, and the impact of on-board HESDs' SOH with different configuration ratios on train operation has also been studied. In cases with an upper limit of the capital cost being 20 k\$, the energy-saving rate and economic cost of different sizes of on-board HESDs are revealed, and the solutions of "Li-ion battery only", "supercapacitor only" and "no on-board HESDs" are used for comparison. When the capital cost is relaxed to be higher than 20 k\$, the optimization performance of the proposed model has been further improved.

Based on the abovementioned case studies, it can be concluded that the energy-saving rate of on-board HESDs are significantly reduced in cases 1-8 with a reduction of supercapacitor investment proportion. From the perspective of the long-term train operation, it is found that the energy-saving rate and economic cost are the optimal solutions at the same time when the investment ratio of the supercapacitor to Li-ion battery is 3:1. Although the degradation cost of the solution of "supercapacitor only" is less than most other cases, its energy-saving rate is not remarkable, which will lead to higher train operating costs during the long-term operation and undermine its energy-saving potential. Furthermore, it can be found that the cost per kilometer dropped from 0.55 USD/km to 0.53 USD/km when the capital investment was relaxed from 20k\$ to 60k\$. In short, based on the proposed method, the optimal sizing of on-board HESDs can be obtained to minimize the overall cost, and railway operators concerned factors, namely the long-term energy consumption of trains under variable capital investment, have also been studied, which further reveals the impact of on-board HESDs with different configuration ratios and different capital investment on the energy-saving effect in electrified railway systems.

In this article, more specific properties, e.g., internal resistance, temperature and charging and discharging control strategies of on-board HESDs under different frequency demand power, which are very important performance metrics in energy management problems, are not considered. In future work, it is our intention to incorporate these performance metrics and verify by hardware-in-the-loop testing for improving the the fineness of the proposed model. Also, through coordinated control of various components of on-board HESDs, the real-time energy split strategy can be further studied based on the proposed model.

REFERENCES

[1] A. González-Gil, R. Palacin, and P. Batty, "Sustainable urban rail systems: Strategies and technologies for optimal management of regenerative braking energy," *Energy Convers. Manag.*, vol. 75, pp. 374–388, Nov. 2013.

[2] S. Vazquez, S. M. Lukic, E. Galvan, L. G. Franquelo, and J. M. Carrasco, "Energy storage systems for transport and grid applications," *IEEE Trans. Ind. Electron.*, vol. 57, no. 12, pp. 3881–3895, Dec. 2010.

[3] T. Ratniyomchai, S. Hillmansen, and P. Tricoli, "Recent developments and applications of energy storage devices in electrified railways," *IET Elect. Syst. Transp.*, vol. 4, no. 1, pp. 9–20, Mar. 2014.

[4] A. Khaligh and Z. Li, "Battery, ultracapacitor, fuel cell, and hybrid energy storage systems for electric, hybrid electric, fuel cell, and plug-in hybrid electric vehicles: State of the art," *IEEE Trans. Veh. Technol.*, vol. 59, no. 6, pp. 2806–2814, Jul. 2010.

[5] N. Ghaviha, J. Campillo, M. Bohlin, and E. Dahlquist, "Review of application of energy storage devices in railway transportation," *Energy Proc.*, vol. 105, pp. 4561–4568, May 2017.

[6] C. C. Chan, A. Bouscayrol, and K. Chen, "Electric, hybrid, and fuel-cell vehicles: Architectures and modeling," *IEEE Trans. Veh. Technol.*, vol. 59, no. 2, pp. 589–598, Feb. 2010.

[7] D. Iannuzzi, F. Ciccarelli, and D. Lauria, "Stationary ultracapacitors storage device for improving energy saving and voltage profile of light transportation networks," *Transp. Res. C, Emerg. Technol.*, vol. 21, no. 1, pp. 321–337, 2012.

[8] R. Hemmati and H. Saboori, "Emergence of hybrid energy storage systems in renewable energy and transport applications—A review," *Renew. Sustain. Energy Rev.*, vol. 65, pp. 11–23, Nov. 2016.

[9] T. S. Babu, K. R. Vasudevan, V. K. Ramachandaramurthy, S. B. Sani, S. Chemud, and R. M. Lajim, "A comprehensive review of hybrid energy storage systems: Converter topologies, control strategies and future prospects," *IEEE Access*, vol. 8, pp. 148702–148721, 2020.

[10] A. González-Gil, R. Palacin, P. Batty, and J. P. Powell, "A systems approach to reduce urban rail energy consumption," *Energy Convers. Manage.*, vol. 80, pp. 509–524, Apr. 2014.

[11] H. Xia, H. Chen, Z. Yang, F. Lin, and B. Wang, "Optimal energy management, location and size for stationary energy storage system in a metro line based on genetic algorithm," *Energies*, vol. 8, no. 10, pp. 11618–11640, 2015.

[12] H. Kobayashi, J. Asano, T. Saito, and K. Kondo, "A power control method to save energy for wayside energy storage systems in dc-electrified railway system," *Elect. Eng. Jpn.*, vol. 196, no. 2, pp. 56–66, 2016.

[13] M. Miyatake and K. Matsuda, "Energy saving speed and charge/discharge control of a railway vehicle with on-board energy storage by means of an optimization model," *IEEJ Trans. Elect. Electron. Eng.*, vol. 4, no. 6, pp. 771–778, Nov. 2009.

[14] C. Wu, S. Lu, F. Xue, L. Jiang, and J. Yang, "Optimization of speed profile and energy interaction at stations for a train vehicle with on-board energy storage device," in *Proc. IEEE Intell. Vehicles Symp. (IV)*, Jun. 2018, pp. 1–6.

[15] C. Wu, W. Zhang, S. Lu, Z. Tan, F. Xue, and J. Yang, "Train speed trajectory optimization with on-board energy storage device," *IEEE Trans. Intell. Transp. Syst.*, vol. 20, no. 11, pp. 4092–4102, Nov. 2019.

[16] Y. Huang, L. Yang, T. Tang, Z. Gao, F. Cao, and K. Li, "Train speed profile optimization with on-board energy storage devices: A dynamic programming based approach," *Comput. Ind. Eng.*, vol. 126, pp. 149–164, Dec. 2018.

[17] J. Snoussi, S. Ben Elghali, M. Benbouzid, and M. F. Mimouni, "Optimal sizing of energy storage systems using frequency-separation-based energy management for fuel cell hybrid electric vehicles," *IEEE Trans. Veh. Technol.*, vol. 67, no. 10, pp. 9337–9346, Oct. 2018.

[18] L. Zhang, X. Hu, Z. Wang, F. Sun, J. Deng, and D. G. Dorrell, "Multiobjective optimal sizing of hybrid energy storage system for electric vehicles," *IEEE Trans. Veh. Technol.*, vol. 67, no. 2, pp. 1027–1035, Feb. 2018.

[19] T. Zhu, R. G. A. Wills, R. Lot, X.-N. Kong, and X. Yan, "Optimal sizing and sensitivity analysis of a battery-supercapacitor energy storage system for electric vehicles," *Energy*, vol. 2, pp. 119–131, Apr. 2021.

[20] Y. Bai, J. Li, H. He, R. C. D. Santos, and Q. Yang, "Optimal design of a hybrid energy storage system in a plug-in hybrid electric vehicle for battery lifetime improvement," *IEEE Access*, vol. 8, pp. 142148–142158, 2020.

[21] M. Kapetanovic, A. Núñez, N. van Oort, and R. M. Goverde, "Reducing fuel consumption and related emissions through optimal sizing of energy storage systems for diesel-electric trains," *Appl. Energy*, vol. 294, pp. 117–128, Jul. 2021.

[22] S. Tang, X. Huang, Q. Li, N. Yang, Q. Liao, and K. Sun, "Optimal sizing and energy management of hybrid energy storage system for high-speed railway traction substation," *J. Electr. Eng. Technol.*, vol. 29, pp. 110–122, May 2021.

[23] D. Roch-Dupré, C. Camacho-Gómez, A. P. Cucala, S. Jiménez-Fernández, L. López, A. Portilla-Figueras, R. R. Pecharromán, A. Fernández-Cardador, and S. Salcedo-Sanz, "Optimal location and sizing of energy storage systems in DC-electrified railway lines using a coral reefs optimization algorithm with substrate layers," *Energies*, vol. 14, pp. 4753–4766, Jan. 2021.

[24] R. Lamedica, A. Ruvio, L. Palagi, and N. Mortelliti, "Optimal siting and sizing of wayside energy storage systems in a DC railway line," *Energies*, vol. 13, pp. 6271–6285, Jan. 2020.

[25] G. Graber, V. Calderaro, V. Galdi, A. Piccolo, R. Lamedica, and A. Ruvio, "Techno-economic sizing of auxiliary-battery-based substations in DC railway systems," *IEEE Trans. Transport. Electrific.*, vol. 4, no. 2, pp. 616–625, Jun. 2018.

[26] S. de la Torre, A. J. Sánchez-Racero, J. A. Aguado, M. Reyes, and O. Martínez, "Optimal sizing of energy storage for regenerative braking in electric railway systems," *IEEE Trans. Power Syst.*, vol. 30, no. 3, pp. 1492–1500, May 2015.

[27] A. Ovalle, J. Pouget, S. Bacha, L. Gerbaud, E. Vinot, and B. Sonier, "Energy storage sizing methodology for mass-transit direct-current way-side support: Application to French railway company case study," *Appl. Energy*, vol. 230, pp. 1673–1684, Nov. 2018.

[28] C. Wu, S. Lu, F. Xue, L. Jiang, and M. Chen, "Optimal sizing of onboard energy storage devices for electrified railway systems," *IEEE Trans. Transport. Electrific.*, vol. 6, no. 3, pp. 1301–1311, Sep. 2020.

[29] C. Wu, B. Xu, S. Lu, F. Xue, L. Jiang, and M. Chen, "Adaptive eco-driving strategy and feasibility analysis for electric trains with onboard energy storage devices," *IEEE Trans. Transport. Electrific.*, vol. 7, no. 3, pp. 1834–1848, Sep. 2021.

[30] H. Rubenbauer and S. Henninger, "Definitions and reference values for battery systems in electrical power grids," *J. Energy Storage*, vol. 12, pp. 87–107, Aug. 2017.

[31] G. Bai, P. Wang, C. Hu, and M. Pecht, "A generic model-free approach for lithium-ion battery health management," *Appl. Energy*, vol. 135, pp. 247–260, Dec. 2014.

[32] J. Bisschop, *Linear Programming Tricks*. The Netherlands: AIMMS, 2006, ch. 6, pp. 63–75.

[33] K. Huang, J. Wu, X. Yang, Z. Gao, F. Liu, and Y. Zhu, "Discrete train speed profile optimization for urban rail transit: A data-driven model and integrated algorithms based on machine learning," *J. Adv. Transp.*, vol. 13, pp. 199–205, Mar. 2019.

[34] S. Koohi-Fayegh and M. A. Rosen, "A review of energy storage types, applications and recent developments," *J. Energy Storage*, vol. 27, pp. 101–119, Feb. 2020.

[35] C. Wu, S. Lu, F. Xue, L. Jiang, M. Chen, and J. Yang, "A two-step method for energy-efficient train operation, timetabling, and onboard energy storage device management," *IEEE Trans. Transport. Electrific.*, vol. 7, no. 3, pp. 1822–1833, Sep. 2021.

[36] H. Yang, W. Shen, Q. Yu, J. Liu, Y. Jiang, E. Ackom, and Z. Y. Dong, "Coordinated demand response of rail transit load and energy storage system considering driving comfort," *CSEE J. Power Energy Syst.*, vol. 6, no. 4, pp. 749–759, Dec. 2020.

[37] B. Xu, J. Zhao, T. Zheng, E. Litvinov, and D. S. Kirschen, "Factoring the cycle aging cost of batteries participating in electricity markets," *IEEE Trans. Power Syst.*, vol. 33, no. 2, pp. 2248–2259, Mar. 2018.

[38] M. Wieczorek, M. Lewandowski, and W. Jefimowski, "Cost comparison of different configurations of a hybrid energy storage system with battery-only and supercapacitor-only storage in an electric city bus," *Bull. Polish Acad. Sci.-Tech. Sci.*, vol. 37, no. 6, pp. 1095–1106, 2019.

[39] M. Ceraolo and G. Lutzemberger, "Stationary and on-board storage systems to enhance energy and cost efficiency of tramways," *J. Power Sources*, vol. 264, pp. 128–139, Oct. 2014.

CHAOXIAN WU was born in Beihai, Guangxi, China, in 1992. He received the B.Eng. degree in traffic engineering from Tongji University, Shanghai, China, the Intercollegiate M.Sc. degree in transport and sustainable development from the Imperial College London, U.K., and University College London, U.K., and the Ph.D. degree in electrical engineering and electronics from the University of Liverpool, U.K. He is currently an Assistant Professor at the School of Systems Science and Engineering, Sun Yat-sen University, Guangzhou, China. His main research interests include railway engineering, train operation optimization, energy-saving strategies in transportation, and smart transportation.

GUANGZHAO MENG was born in Jingzhou, Hubei, China, in 1997. He received the B.S. degree from the Wuhan Institute of Technology, Hubei. He is currently pursuing the M.S. degree with the Shien-Ming Wu School of Intelligent Engineering, South China University of Technology, China. His main research interests include hydrogen railway engineering, energy management, and energy-saving strategies.

FEI XUE received the bachelor's and master's degrees in power system and its automation from Wuhan University, in 1999 and 2002, respectively, and the Ph.D. degree in electrical engineering from the Politecnico di Torino, Italy, in 2009. He was a former Senior Researcher on eco-city at Siemens. He has been involved in designing and implementing the operating system for electric vehicle service network with the State Grid Corporation of China, as well as several research projects on security of critical infrastructures supported by the European Commission and NATO. His research interests include networking operation for electric vehicles, eco-city, security of critical infrastructures, and energy internet.

BOLUN ZHANG received the M.S. degree in electrical engineering from the Hunan University of Technology, Zhuzhou, China, in 2019. He is currently pursuing the Ph.D. degree with the Shien-Ming Wu School of Intelligent Engineering, South China University of Technology, Guangzhou, China. His main research interests include energy storage technology, train optimal control, and energy management in electrified transportation.

SHAOFENG LU received the B.Eng. degree (Hons.) from the University of Birmingham, in 2007, the B.Eng. degree from the Huazhong University of Science and Technology, Wuhan, China, in 2007, and the Ph.D. degree from the University of Birmingham, in 2011. He is currently an Associate Professor with the Shien-Ming Wu School of Intelligent Engineering (WUSIE), South China University of Technology (SCUT), China. Before joining SCUT in 2019, he spent six years as a Faculty Member with the Department of Electrical and Electronic Engineering, Xi'an Jiaotong-Liverpool University (XJTLU), China. His main research interests include power management strategies, railway traction systems, electric vehicles, optimization techniques, and energy-efficient transportation systems.

• • •